

## Triple-junction thin-film silicon solar cell fabricated on periodically textured substrate with a stabilized efficiency of 13.6%

Hitoshi Sai (齋 均), Takuya Matsui (松井 卓矢), Takashi Koida (鯉田 崇), Koji Matsubara (松原 浩司), Michio Kondo (近藤 道雄), Shuichiro Sugiyama (杉山 秀一郎), Hirotaka Katayama (片山 博貴), Yoshiaki Takeuchi (竹内 良昭), and Isao Yoshida (吉田 功)

Citation: *Appl. Phys. Lett.* **106**, 213902 (2015);

View online: <https://doi.org/10.1063/1.4921794>

View Table of Contents: <http://aip.scitation.org/toc/apl/106/21>

Published by the American Institute of Physics

---

### Articles you may be interested in

[Stabilized 14.0%-efficient triple-junction thin-film silicon solar cell](#)

*Applied Physics Letters* **109**, 183506 (2016); 10.1063/1.4966996

[Detailed Balance Limit of Efficiency of p-n Junction Solar Cells](#)

*Journal of Applied Physics* **32**, 510 (2004); 10.1063/1.1736034

[A 2-terminal perovskite/silicon multijunction solar cell enabled by a silicon tunnel junction](#)

*Applied Physics Letters* **106**, 121105 (2015); 10.1063/1.4914179

[Amorphous silicon solar cell](#)

*Applied Physics Letters* **28**, 671 (2008); 10.1063/1.88617

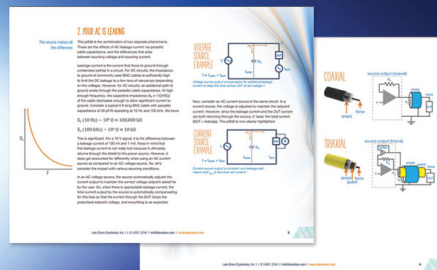
[19.8% efficient "honeycomb" textured multicrystalline and 24.4% monocrystalline silicon solar cells](#)

*Applied Physics Letters* **73**, 1991 (1998); 10.1063/1.122345

[The efficiency limit of  \$\text{CH}\_3\text{NH}\_3\text{PbI}\_3\$  perovskite solar cells](#)

*Applied Physics Letters* **106**, 221104 (2015); 10.1063/1.4922150

---



## 5 Electronic Measurement Pitfalls to Avoid

Get the whitepaper

# Triple-junction thin-film silicon solar cell fabricated on periodically textured substrate with a stabilized efficiency of 13.6%

Hitoshi Sai (齋 均),<sup>1,a)</sup> Takuya Matsui (松井 卓矢),<sup>1</sup> Takashi Koida (鯉田 崇),<sup>1</sup> Koji Matsubara (松原 浩司),<sup>1</sup> Michio Kondo (近藤 道雄),<sup>2</sup> Shuichiro Sugiyama (杉山 秀一郎),<sup>3</sup> Hirotaka Katayama (片山 博貴),<sup>4</sup> Yoshiaki Takeuchi (竹内 良昭),<sup>5</sup> and Isao Yoshida (吉田 功)<sup>6</sup>

<sup>1</sup>Research Center for Photovoltaic Technologies, National Institute of Advanced Industrial Science and Technology (AIST), Central 2, Umezono 1-1-1, Tsukuba, Ibaraki 305-8568, Japan

<sup>2</sup>Fukushima Renewable Energy Research Institute, National Institute of Advanced Industrial Science and Technology (AIST), 2-2-9 Machiikedai, Koriyama, Fukushima 963-0298, Japan

<sup>3</sup>Sharp Corporation, 282-1 Hajikami, Katsuragi, Nara 639-2198, Japan

<sup>4</sup>Panasonic Corporation, Kadoma, Osaka 571-8686, Japan

<sup>5</sup>Mitsubishi Heavy Industries Ltd., Isahaya, Nagasaki 854-0065, Japan

<sup>6</sup>Photovoltaic Power Generation Technology Research Association (PVTEC), Tsukuba 305-8568, Japan

(Received 12 April 2015; accepted 18 May 2015; published online 28 May 2015)

We report a high-efficiency triple-junction thin-film silicon solar cell fabricated with the so-called substrate configuration. It was verified whether the design criteria for developing single-junction microcrystalline silicon ( $\mu\text{c-Si:H}$ ) solar cells are applicable to multijunction solar cells. Furthermore, a notably high short-circuit current density of  $32.9 \text{ mA/cm}^2$  was achieved in a single-junction  $\mu\text{c-Si:H}$  cell fabricated on a periodically textured substrate with a high-mobility front transparent contacting layer. These technologies were also combined into a-Si:H/ $\mu\text{c-Si:H}$ / $\mu\text{c-Si:H}$  triple-junction cells, and a world record stabilized efficiency of 13.6% was achieved. © 2015 AIP Publishing LLC. [<http://dx.doi.org/10.1063/1.4921794>]

Thin-film silicon solar cells (TFSSCs) had been commercialized in the 1970s; they are used in a wide variety of applications from large-area photovoltaic systems to consumer products. The main challenge in TFSSCs is the improvement in power conversion efficiency (PCE). To date, an initial PCE of 16.3% (Ref. 1) has been reported in a triple-junction cell, using hydrogenated amorphous silicon (a-Si:H), amorphous silicon germanium (a-SiGe:H), and microcrystalline silicon ( $\mu\text{c-Si:H}$ ). However, the highest stabilized efficiency reported is 13.4% (Ref. 2) because of the light-induced degradation phenomena.<sup>3</sup>

It is known that  $\mu\text{c-Si:H}$  has higher tolerance to light soaking than pure amorphous materials.<sup>4</sup> In recent years, the PCE of single-junction  $\mu\text{c-Si:H}$  solar cells steadily improved from 10.1% to 11.8%.<sup>5–8</sup> This improvement in PCE was triggered by the introduction of well-designed textured substrates with a hexagonal dimple array for achieving better light trapping.<sup>9,10</sup> Hereafter, we refer to these periodically textured substrates as the “honeycomb-textured substrates.” In this study, we applied honeycomb-textured substrates to multijunction TFSSCs.

The details of the fabrication procedure of honeycomb textured substrates were reported elsewhere.<sup>9,10</sup> All Si-related layers including a-Si:H,  $\mu\text{c-Si:H}$ , and *p*- and *n*-type doped layers were grown with plasma-enhanced chemical vapor deposition (PECVD) at temperatures of 140–200 °C, using  $\text{SiH}_4$ ,  $\text{H}_2$ ,  $\text{B}_2\text{H}_6$ ,  $\text{PH}_3$ , and  $\text{CO}_2$  as source gases. Most of the layers were grown with a laboratory-scale PECVD, unless noted otherwise. As a front window electrode, transparent conductive oxide (TCO) films of  $\text{In}_2\text{O}_3\text{:Sn}$  (ITO) or  $\text{In}_2\text{O}_3\text{:H}$  (IOH)<sup>11</sup> were deposited using radio frequency (RF)

magnetron sputtering at room temperature, followed by post annealing at 175 °C. For some solar cells, an antireflection (AR) film based on the moth-eye structure<sup>12</sup> was applied to suppress the reflection loss. Cell performance was evaluated by measuring current density-voltage (*J-V*) characteristics under air mass 1.5G ( $100 \text{ mW/cm}^2$ ), with a dual-light solar simulator (Wacom Electric, WXS-50 S-L2). Open-circuit voltage ( $V_{\text{OC}}$ ),  $J_{\text{SC}}$ , fill factor (FF), and PCE were also recorded. External quantum efficiency (EQE) spectra were measured with a Bunkou-Keiki, CEP-25BXS setup. The reflectivity (*R*) of the cells was also measured using a spectrometer with an integral sphere (Perkin Elmer, Lambda 950). Absorption values were simply obtained by calculating  $1 - R$ .

In previous reports, it was pointed out that in order to avoid defective areas formation within the  $\mu\text{c-Si:H}$  layers, the period of honeycomb textures should be controlled to satisfy  $P \sim t_i$ , where *P* and *t<sub>i</sub>* are the period of honeycomb textures and the thickness of  $\mu\text{c-Si:H}$  layers, respectively.<sup>10</sup> In this study, we focus on a-Si:H/ $\mu\text{c-Si:H}$ / $\mu\text{c-Si:H}$  triple-junction cells in the so-called substrate configuration. The design criterion of single-junction cells is expected to be applicable to the triple-junction cells, as approximately 90% of the total thickness is occupied by the middle and bottom  $\mu\text{c-Si:H}$  cells. However, in the case of multijunction cells, the growth of  $\mu\text{c-Si:H}$  layers is interrupted by doped layers or intermediate reflectors, such as nanocrystalline silicon oxide (nc-SiO<sub>x</sub>:H) film.<sup>13</sup> To address the impact of the interruption and insertion of other layers between  $\mu\text{c-Si:H}$  films, the film stacks of  $\mu\text{c-Si:H}$ /nc-SiO<sub>x</sub>:H layers were deposited and investigated.

Fig. 1(a) shows a top scanning electron microscope (SEM) image of the honeycomb-textured substrate with

<sup>a)</sup>Email: [sai@aist.go.jp](mailto:sai@aist.go.jp)

$P = 1.5 \mu\text{m}$ . It is clear that many concaves are arranged in a honeycomb structure. Each concave has a flat bottom part and an aspect ratio of  $H/P = 0.25$ , where  $H$  denotes the texture peak height. Hence, we prepared honeycomb-textured substrates with  $P = 1.5, 2.5$ , and  $3.5 \mu\text{m}$ , and deposited a triple stack of nc-SiO<sub>x</sub>:H/ $\mu\text{c-Si:H}$  layers (30 nm/0.9  $\mu\text{m}$ ) on the substrates. Figs. 1(b)–1(d) shows the cross-sectional transmission electron microscope (TEM) images of the nc-SiO<sub>x</sub>:H/ $\mu\text{c-Si:H}$  film stacks along the XX' line shown in Fig. 1(a). In Figs. 1(b)–1(d), the film stack surface morphology evolution is well visualized with the insertion of nc-SiO<sub>x</sub>:H layers, which is indicated by thin bright lines in this figure. It is clear that the  $\mu\text{c-Si:H}$  film is grown normal to the local surfaces, even after the growth interruption owing to nc-SiO<sub>x</sub>:H insertion. It is also found that the flat bottom part of each concave gradually shrinks during  $\mu\text{c-Si:H}$  film growth. In the case of  $P = 1.5 \mu\text{m}$  (Fig. 1(b)), a crack propagating through the nc-SiO<sub>x</sub>:H layer is clearly observed in the upper half of the film, which is indicated by black arrows. The crack starts to grow just after the flat bottom part vanishes, and hence, a funnel-shaped hole is formed. Furthermore, the nc-SiO<sub>x</sub>:H film is not clearly visible near the crack, suggesting that layer-by-layer growth is hampered. However, as indicated in Fig. 1(c)–1(d), the crack formation can be either suppressed or prevented by increasing the value of  $P$ . The crack formation is most likely caused by the shadowing effect at the funnel-shaped holes where there is insufficient film precursor supply during the film growth. These results are in good agreement with those obtained in single-junction  $\mu\text{c-Si:H}$  solar cells.<sup>10</sup> Therefore, we conclude that the growth of  $\mu\text{c-Si:H}$  film on textured substrates is not severely affected by the insertion of other thin layers.

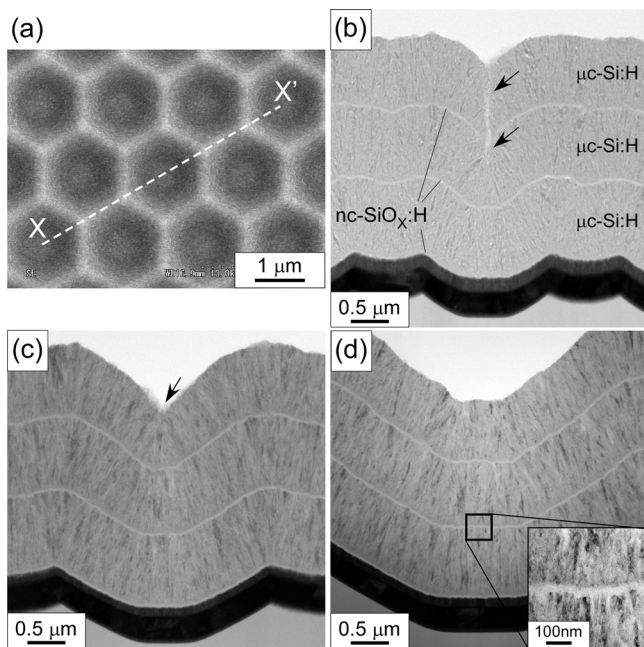


FIG. 1. Topological images of nc-SiO<sub>x</sub>:H/ $\mu\text{c-Si:H}$  film stacks on honeycomb textures. (a) Top SEM view of a honeycomb substrate with  $P = 1.5 \mu\text{m}$ , cross-sectional TEM images of  $\mu\text{c-Si:H}$ /nc-SiO<sub>x</sub> stacks on honeycomb textures with (b)  $P = 1.5 \mu\text{m}$ , (c)  $P = 2.5 \mu\text{m}$ , and (d)  $P = 3.5 \mu\text{m}$ . The white dashed line in (a) indicates the slicing direction for making TEM samples. Black arrows in (b) and (c) indicate a crack or defective area.

Based on the aforementioned findings, we focused on the  $J_{\text{SC}}$  enhancement of the bottom  $\mu\text{c-Si:H}$  cell, which governs the total photocurrent density in a multijunction cell. In a previous study, we reported  $J_{\text{SC}} = 30.8 \text{ mA/cm}^2$  (in an active area) for a single-junction  $\mu\text{c-Si:H}$  cell with  $(P, t_i) = (3 \mu\text{m}, 3 \mu\text{m})$  and IOH front contact.<sup>14</sup> However, in multijunction cells, parasitic absorption loss is inevitably increased owing to the increased number of doped layers. Thus, in this research, thicker  $\mu\text{c-Si:H}$  cells with  $(P, t_i) = (4 \mu\text{m}, 4 \mu\text{m})$  are developed. The device structure is a honeycomb-textured substrate/Ag/GZO/(n)nc-SiO<sub>x</sub>:H/(i) $\mu\text{c-Si:H}$ /buffer/(p)nc-SiO<sub>x</sub>:H/TCO layer/Ag grid, from the bottom to the top. Note that the (i) $\mu\text{c-Si:H}$  layer was deposited with a very high frequency (VHF) PECVD tool at a deposition rate of 1 nm/s.<sup>8</sup> EQE spectra of two  $\mu\text{c-Si:H}$  cells with ITO and IOH front contacts are compared in Fig. 2. Both cells have moderate active-area PCEs of 9.5%–10%. As shown in Fig. 2, both cells exhibit  $J_{\text{SC}} > 31 \text{ mA/cm}^2$ , indicating a superior light trapping effect by the honeycomb texture. In addition, by using IOH,  $J_{\text{SC}}$  was increased up to  $32.9 \text{ mA/cm}^2$  mainly because of the suppressed free carrier absorption (FCA) in the infrared (IR) region. This is confirmed by the relatively small gap between the EQE and the absorption spectra in the IR region, as shown in Fig. 2. It should be also stressed out that a noteworthy photocurrent density of  $34.1 \text{ mA/cm}^2$  is obtained when the carrier collection is supported by a reverse bias voltage during the EQE measurement.

Next, we compare our experimental results with the ideal absorption spectrum of a c-Si slab at the so-called Lambertian limit.<sup>15</sup> The absorbance ( $A$ ) at the Lambertian limit was simply calculated by the formula<sup>16</sup>

$$A = \alpha(\lambda) / \{ \alpha(\lambda) + 1 / (4n^2d) \}, \quad (1)$$

where  $\alpha(\lambda)$  is the absorption coefficient of c-Si,  $n(\lambda)$  is the refractive index, and  $d$  is the thickness of c-Si slab (here,  $4 \mu\text{m}$ ). As seen in Fig. 2, the biased EQE spectrum of the cell is relatively closer to the Lambertian limit. Nevertheless, there are significant gaps between the experimental and the ideal absorption spectra. The ideal absorption curve provides a potential current density of  $36.9 \text{ mA/cm}^2$ . Therefore, the

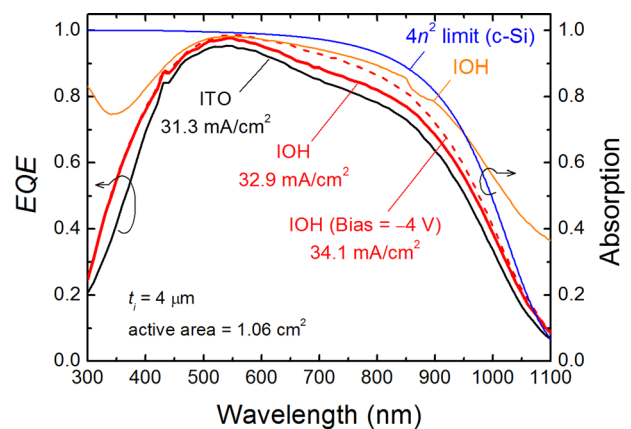


FIG. 2. EQE and absorption spectra of  $\mu\text{c-Si:H}$  cells on a honeycomb-textured substrate with  $(P, t_i) = (4 \mu\text{m}, 4 \mu\text{m})$ , with ITO or IOH front contact layer. The ideal absorption curve of c-Si slab ( $d = 4 \mu\text{m}$ ) at the Lambertian limit ( $4n^2$  limit) is also plotted for comparison.

TABLE I. Photovoltaic parameters of the record a-Si:H/ $\mu$ c-Si:H/ $\mu$ c-Si:H triple-junction solar cells. The cell has a designated area of 1.045 cm<sup>2</sup> and an AR film on the top.

	$V_{OC}$ (V)	$J_{SC}$ (mA/cm <sup>2</sup> )	FF	PCE (%)	Measurement
Initial	1.907	9.7	0.780	14.5	In-house
Light soaked	1.904	9.8	0.745	13.8	In-house
$\Delta\%$	-0.18	+0.23	-4.47	-4.42	
Light soaked	1.901	9.92	0.721	13.6	Certified

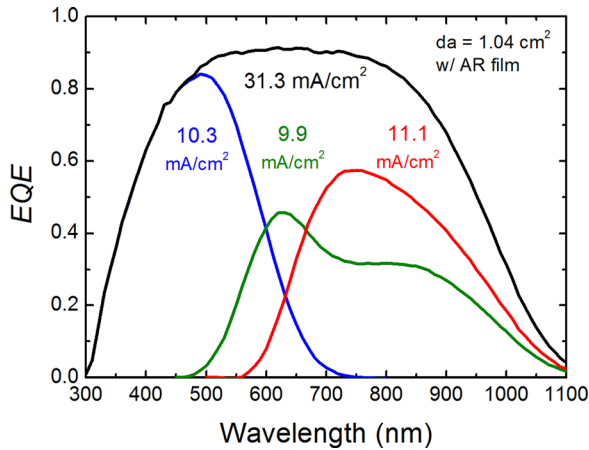


FIG. 3. EQE spectra of the record a-Si:H/ $\mu$ c-Si:H/ $\mu$ c-Si:H triple-junction solar cell after light soaking. The cell has a designated area of 1.045 cm<sup>2</sup> and an AR film on the top.

optical design of the current  $\mu$ c-Si:H cell still has a large room for improvement.

The development of high-efficiency a-Si:H solar cells is one of the key issues for making high-efficiency multijunction TFSSCs. Recently, we realized a high initial and stabilized designated-area PCEs of 11.3% and 10.2% ( $V_{OC}$  = 0.896 V,  $J_{SC}$  = 16.4 mA/cm<sup>2</sup>, FF = 0.698), respectively, using the triode PECVD technique.<sup>17</sup> However, it is not easy to transfer the technology used in the superstrate configuration to the substrate configuration. To date, we have obtained initial and stabilized active-area PCEs of 10% and 8.5% ( $V_{OC}$  = 0.895 V,  $J_{SC}$  = 15.1 mA/cm<sup>2</sup>, FF = 0.624),

in a substrate-type *n-i-p* a-Si:H cell. The device structure used in this study is Asahi-VU/Ag/GZO/(n)a-Si:H/(i)a-Si:H ( $t_i$  = 250 nm)/buffer/(p)nc-SiO<sub>x</sub>:H/IOH/Ag grid from the bottom to the top. Efficiencies are bottlenecked mainly by low  $J_{SC}$  and FF values, even though the best triode PECVD material has not been applied yet. This topic is currently under investigation.

The aforementioned technologies for *n-i-p*  $\mu$ c-Si:H and a-Si:H cells were applied to a-Si:H/ $\mu$ c-Si:H/ $\mu$ c-Si:H triple-junction cells. The device structure is as follows: honeycomb-textured substrate/Ag/GZO/bottom  $\mu$ c-Si:H cell (VHF-PECVD)/middle  $\mu$ c-Si:H cell/top a-Si:H cell/IOH/Ag grid/AR film, from the bottom to the top. In order to achieve a high  $J_{SC}$ , the total thickness of the active layers was set to approximately 4  $\mu$ m, with a honeycomb-textured substrate with  $P$  = 4  $\mu$ m. The  $t_i$  of the top, middle, and bottom cells are 250 nm, 1.7  $\mu$ m, and 2.1  $\mu$ m, respectively. Light soaking was performed under the standard condition of 1 Sun at 50 °C, for 1000 h. As a result, we obtained a triple-junction cell with initial and stabilized efficiencies of 14.5% and 13.8%, respectively (Table I). The efficiency degradation by light soaking is mitigated to be as low as 4.4%. This minimized light-induced degradation is attributable to the following two factors. First, this triple-junction cell has two  $\mu$ c-Si:H sub-cells that barely showed any light-induced degradation. Second, the  $J_{SC}$  of this triple-junction cell is limited by the middle  $\mu$ c-Si:H cell. It is known that  $J_{SC}$  being limited by the  $\mu$ c-Si:H cell leads to less light-induced degradation in a-Si:H/ $\mu$ c-Si:H tandem cells.<sup>18</sup> Similarly, in this triple-junction cell, the middle  $\mu$ c-Si:H cell produces the lowest current density of 9.9 mA/cm<sup>2</sup> (Fig. 3).

The best-efficiency cell was also independently characterized by the Characterization, Standard and Measurement team of the Research Center for Photovoltaic Technologies, National Institute of Advanced Industrial Science and Technology (AIST CSM team). A stabilized PCE of 13.6% has been confirmed as shown in Fig. 4 and Table I, which is higher than the record stabilized PCE for TFSSCs reported by Kim *et al.* ( $V_{OC}$  = 1.963 V,  $J_{SC}$  = 9.52 mA/cm<sup>2</sup>, FF = 0.719, PCE = 13.44%).<sup>2</sup> The triple-junction cell designed in this study exhibits a considerable 4% increment in  $J_{SC}$ , which

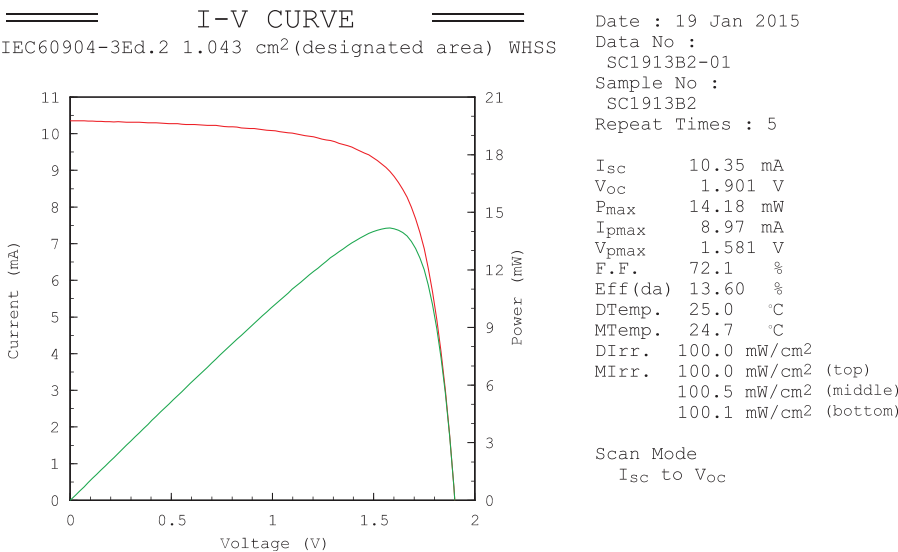


FIG. 4. I-V curve of the record a-Si:H/ $\mu$ c-Si:H/ $\mu$ c-Si:H triple-junction solar cell independently confirmed by the AIST CSM team.



originates from the enhanced light trapping and the suppressed FCA. As a total current density of  $31.3 \text{ mA/cm}^2$  was obtained as shown in Fig. 3, the  $J_{\text{SC}}$  can be further increased up to  $10.4 \text{ mA/cm}^2$  (+5%) simply by balancing the current densities among the subcells. On the other hand, this solar cell shows an inferior  $V_{\text{OC}}$ . We ascribe this to the limited  $V_{\text{OC}}$  in the top a-Si:H cell;  $V_{\text{OC}} > 0.94 \text{ V}$  was reported for the state-of-the-art *n-i-p* a-Si:H cells.<sup>19</sup> When compared with the data obtained at our laboratory, a relatively large discrepancy was found in FF (0.745 and 0.721), which leads to a slightly lower efficiency. We ascribe this discrepancy to the spectral mismatch between the dual-light solar simulator used at our laboratory and the highly accurate triple-light solar simulator used by the AIST CSM team. In fact, the spectrum obtained from our solar simulator is richer in the blue wavelengths than that from the triple-light solar simulator used by the AIST CSM team.

In summary, our original honeycomb-textured substrates were applied to single-junction and multijunction TFSSCs in the substrate configuration. A remarkably high  $J_{\text{SC}}$  of approximately  $33 \text{ mA/cm}^2$  was achieved in a single-junction  $\mu\text{c-Si:H}$  cell having IOH front contact. Furthermore, design criterion in TFSSCs on honeycomb-textured substrates, namely,  $P \sim t_i$ , is applicable not only to single-junction  $\mu\text{c-Si:H}$  cells but also to multijunction TFSSCs having  $\mu\text{c-Si:H}$  subcells. These technologies have been applied to a-Si:H/ $\mu\text{c-Si:H}$  triple-junction cells. Accordingly, a world record stabilized PCE of 13.6% was independently confirmed by the AIST CSM team, despite the limited performance in the top a-Si:H cell and the relatively large current mismatch. Improvements in these aspects will lead to a stabilized PCE exceeding 14% in the near future.

The authors acknowledge Dr. Hishikawa and Ms. Sasaki of AIST CSM team, Dr. Suezaki of Kaneka Corporation, and all thin-film Si consortium members in PVTEC for their great support. This work was supported by New Energy and Industrial Technology Development Organization (NEDO),

Japan. Photolithography process was conducted at the AIST Nano-Processing Facility.

- <sup>1</sup>B. Yan, G. Yue, L. Sivec, F. Yang, and S. Guha, *Appl. Phys. Lett.* **99**, 113512 (2011).
- <sup>2</sup>S. Kim, J.-W. Chung, H. Lee, J. Park, Y. Heo, and H.-M. Lee, *Sol. Energy Mater. Sol. Cells* **119**, 26 (2013).
- <sup>3</sup>D. L. Staebler and C. R. Wronski, *Appl. Phys. Lett.* **31**, 292 (1977).
- <sup>4</sup>J. Meier, R. Flückiger, H. Keppner, and A. Shah, *Appl. Phys. Lett.* **65**, 860 (1994).
- <sup>5</sup>K. Yamamoto, *IEEE Trans. Electron Devices* **46**, 2041 (1999).
- <sup>6</sup>S. Hänni, G. Bugnon, G. Parascandolo, M. Boccard, J. Escarré, M. Despeisse, F. Meillaud, and C. Ballif, *Prog. Photovolt: Res. Appl.* **21**(5), 821 (2013).
- <sup>7</sup>H. Sai, T. Matsui, K. Matsubara, M. Kondo, and I. Yoshida, *IEEE J. Photovolt.* **4**, 1349 (2014).
- <sup>8</sup>H. Sai, K. Maejima, T. Matsui, T. Koida, M. Kondo, S. Nakao, Y. Takeuchi, H. Katayama, and I. Yoshida, "High-efficiency microcrystalline silicon solar cells on honeycomb textured substrates grown with high-rate VHF plasma-enhanced chemical vapor deposition" *Jpn. J. Appl. Phys.* (in press).
- <sup>9</sup>H. Sai, K. Saito, and M. Kondo, *Appl. Phys. Lett.* **101**, 173901 (2012).
- <sup>10</sup>H. Sai, K. Saito, N. Hozuki, and M. Kondo, *Appl. Phys. Lett.* **102**, 053509 (2013).
- <sup>11</sup>T. Koida, H. Fujiwara, and M. Kondo, *Jpn. J. Appl. Phys., Part 2* **46**, L685 (2007).
- <sup>12</sup>H. Sai, T. Matsui, K. Saito, M. Kondo, and I. Yoshida, "Photocurrent enhancement in thin-film silicon solar cells by combination of anti-reflective sub-wavelength structures and light-trapping textures," *Prog. Photovoltaics: Res. Appl.* (published online).
- <sup>13</sup>P. Buehlmann, J. Bailat, D. Dominé, A. Billet, F. Meillaud, A. Feltrin, and C. Ballif, *Appl. Phys. Lett.* **91**, 143505 (2007).
- <sup>14</sup>H. Sai, T. Koida, T. Matsui, I. Yoshida, K. Saito, and M. Kondo, *Appl. Phys. Express* **6**, 104101 (2013).
- <sup>15</sup>E. Yablonovitch, *J. Opt. Soc. Am.* **72**, 899 (1982).
- <sup>16</sup>T. Tiedje, E. Yablonovitch, G. D. Cody, and B. G. Brooks, *IEEE Trans. Electron Devices* **31**, 711 (1984).
- <sup>17</sup>T. Matsui, K. Maejima, A. Bidiville, H. Sai, T. Koida, T. Suezaki, M. Matsumoto, K. Saito, I. Yoshida, and M. Kondo, "High-efficiency thin-film silicon solar cells realized by integrating stable a-Si:H absorbers into improved device design" *Jpn. J. Appl. Phys.* (in press).
- <sup>18</sup>M. Boccard, M. Despeisse, J. Escarré, X. Niquille, G. Bugnon, S. Hänni, M. Bonnet-Eymard, F. Meillaud, and C. Ballif, *IEEE J. Photovoltaics* **4**, 1368 (2014).
- <sup>19</sup>R. Biron, C. Pahud, F.-J. Haug, J. Escarré, K. Söderström, and C. Ballif, *J. Appl. Phys.* **110**, 124511 (2011).